Amino Acids (2012) 43:431–445
DOI 10.1007/s00726-011-1099-4

ORIGINAL ARTICLE

Potential benefits of taurine in the prevention of skeletal muscle impairment induced by disuse in the hindlimb-unloaded rat

Sabata Pierno · Antonella Liantonio · Giulia M. Camerino · Michela De Bellis · Maria Cannone · Gianluca Gramegna · Antonia Scaramuzzi · Simonetta Simonetti · Grazia Paola Nicchia · Davide Basco · Maria Svelto · Jean-François Desaphy · Diana Conte Camerino

Received: 7 February 2011 / Accepted: 20 September 2011 / Published online: 11 October 2011

Abstract Hindlimb unloading (HU) in rats induces severe atrophy and a slow-to-fast phenotype transition in postural slow-twitch muscles, as occurs in human disuse conditions, such as spaceflight or bed rest. In rats, a reduction of soleus muscle weight and a decrease of cross-sectional area (CSA) were observed as signs of atrophy. An increased expression of the fast-isoform of myosin heavy chain (MHC) showed the phenotype transition. In parallel the resting cytosolic calcium concentration (restCa) was decreased and the resting chloride conductance (gCl), which regulates muscle excitability, was increased toward the values of the fast-twitch muscles. Here, we investigated the possible role of taurine, which is known to modulate calcium homeostasis and gCl, in the restoration of muscle impairment due to 14-days-HU. We found elevated taurine content and higher expression of the taurine transporter TauT in the soleus muscle as compared to the fast-twitch extensor digitorum longus (EDL) muscle of control rats. Taurine level was reduced in the HU soleus muscle, although, TauT expression was not modified. Taurine oral supplementation (5 g/kg) fully prevented this loss, and preserved resting gCl and restCa together with the slow MHC phenotype. Taurine supplementation did not prevent the HU-induced drop of muscle weight or fiber CSA, but it restored the expression of MURF-1, an atrophy-related gene, suggesting a possible early protective effect of taurine. In conclusion, taurine prevented the HU-induced phenotypic transition of soleus muscle and might attenuate the atrophic process. These findings argue for the beneficial use of taurine in the treatment of disuse-induced muscle dysfunction.

Keywords Taurine · Slow- and fast-twitch skeletal muscle · Hindlimb unloading · Atrophy · Resting chloride conductance · Resting intracellular calcium

S. Pierno, A. Liantonio and G. M. Camerino contributed equally to this work as first author. J.-F. Desaphy and D. C. Camerino as senior author.

S. Pierno (✉) · A. Liantonio · G. M. Camerino · M. De Bellis · M. Cannone · G. Gramegna · A. Scaramuzzi · J.-F. Desaphy · D. C. Camerino
Section of Pharmacology, Department of Pharmacobiology, University of Bari "Aldo Moro", Via Orabona 4, 70124 Bari, Italy
e-mail: spierno@farmbiol.uniba.it

S. Simonetti
Metabolic Disease Unit, Paediatric Hospital Giovanni XXIII, Via Amendola, 70125 Bari, Italy

G. P. Nicchia · D. Basco · M. Svelto
Department of General and Environmental Physiology, University of Bari "Aldo Moro", Via Orabona 4, 70124 Bari, Italy

Introduction

Impairment of skeletal muscle function due to disuse

During spaceflight, prolonged bed rest, or the aging process, human subjects experience severe alterations in skeletal muscle function, which result in a reduction of strength and locomotion ability (Pavy-Le Traon et al. 2007). Muscle disuse preferentially affects the postural muscles, such as the slow-twitch soleus muscle. These muscles undergo an atrophic process and a slow-to-fast phenotype transition, which represent an adaptation of the muscles to the reduced activity (Talmadge 2000). As a result, the muscles are unable to function correctly upon return to normal activity, and this may contribute to

morbidity. A full understanding of the mechanisms of disuse-induced muscle atrophy in humans is incomplete (Fitts et al. 2001) and at the moment, few molecules have been proposed for therapy. When possible, specific exercise protocols are frequently used but show only limited benefits to prevent muscle dysfunction. It has been shown that supplementation with essential amino acids and carbohydrates in combination with exercise attenuates muscle protein loss in humans during prolonged inactivity (Paddon-Jones et al. 2004; Fitts et al. 2007). Drugs for preventive or curative purposes are not yet available (Adams et al. 2003).

Cellular targets of disuse in a hindlimb-unloaded animal model

A widely accepted model for muscle disuse is the hindlimb-unloaded (HU) rat, a ground-based animal model that mimics microgravity conditions (Morey-Holton et al. 2005). As in humans (Fitts et al. 2010), the soleus muscle of HU rats becomes atrophic and enters a partial slow-to-fast phenotype transition, that is characterized by an increased expression of fast myosin heavy chain (MHC) isoforms and of metabolic proteins required for fast-twitch contraction (Schulte et al. 1993; Harridge 2007). Also muscle ion channels are critical determinants of the muscle phenotype, because they control excitability and excitation/contraction coupling, and modulate contraction and gene expression. We previously found important modifications of ion channel function and expression during HU, which were mainly in accordance with the phenotype transition (Desaphy et al. 2001, 2005; Frigeri et al. 2001; Pierno et al. 2002, 2007; Fraysse et al. 2003; Tricarico et al. 2005). The expression of the ClC-1 chloride channel, which is responsible for the resting chloride conductance of sarcolemma, is greater in fast-twitch muscles compared to slow-twitch muscles (Steinmeyer et al. 1991; Pierno et al. 1999). Thus, chloride conductance (gCl) controls the electrical stability of sarcolemma. The lower gCl found in soleus muscle is thought to be responsible for the increase in muscle excitability and the resistance to fatigue that is typical of postural muscles (Pedersen et al. 2005, 2009; Pierno et al. 2007). After 1–3 weeks of HU, the gCl increases in soleus muscle toward a value more similar to a fast-twitch muscle, and this is due to the increased expression of ClC-1 channels (Pierno et al. 2002). In addition the cytosolic concentration of resting calcium (restCa) depends on the muscle phenotype. The restCa concentration is higher in the soleus muscle compared to EDL muscles, and it was found to be decreased in HU soleus muscle (Fraysse et al. 2003). The reduced restCa concentration likely contributes to the positive shift of the mechanical threshold (MT), a functional index of excitation–contraction coupling, observed in HU soleus muscle. Interestingly, the changes in the levels of gCl and restCa were observed after 3 days of HU, at which point the expression of the fast MHC-positive fibers in the HU soleus muscle remained unchanged at both the mRNA and protein level (Pierno et al. 2002). We have demonstrated that this early change of gCl is attributable to a reduced activity of protein kinase C (PKC), which is important in the regulation of the ClC-1 channel activity (Pierno et al. 2007). These findings suggest that gCl and restCa are early determinants of soleus muscle adaptation to reduced activity and therefore represent suitable drug targets to counteract the dysfunction of disused muscle.

Taurine as a potential countermeasure for muscle disuse

Taurine is a sulfonic amino acid prevalent in excitable tissues that has been proposed to protect muscle function in a variety of diseases through diverse mechanisms (Huxtable 1992). Taurine is considered to be a membrane stabilizer because it controls muscle excitability through direct or PKC-mediated modulation of ClC-1 chloride channel or of others membrane ion channels (Conte Camerino et al. 2004). Taurine also modulates intracellular calcium homeostasis which is important for controlling muscle fiber contractility (Huxtable 1992). To support the role of this essential amino acid in skeletal muscle function different studies have shown that a reduction in tissue taurine content induced by pharmacological treatment or genetic manipulation leads to alterations of skeletal muscle function (Warskulat et al. 2004; Hamilton et al. 2006; Ito et al. 2008). We have also demonstrated that the taurine content is reduced in the fast-twitch muscles of aged rats, which are characterized by sarcopenia. However, taurine supplementation improved the muscle function (Pierno et al. 1998). To date, it is unknown whether taurine content is altered in humans during muscle inactivity or whether taurine supplementation would improve muscle function. To our knowledge, only one report published by NASA has shown that large amounts of taurine were excreted in the urine of the astronauts of the APOLLO mission (Leach et al. 1975). Thus, our study in the HU rat may be beneficial as a preclinical study of the efficacy of taurine in skeletal muscle damage due to disuse. Because taurine does not cause negative side effects it can be used at high doses. It has been shown that the administration of similar or higher doses of taurine than those used in this study are safe and display protective effects in different physiopathological situations (Yokogoshi et al. 1999; Yokogoshi and Oda 2002; Yang et al. 2004). Because taurine is highly concentrated in the myocytes, it is important to use high doses to allow the amino acid to reach the intracellular regions (Huxtable 1992). Interestingly, there is twice as

much taurine in the soleus muscle than in the fast-twitch muscles, which suggests that the taurine content depends on the muscle phenotype (Iwata et al. 1986; Yoshioka et al. 2002; Dawson et al. 2002). However, the functional relevance of this difference has not been clarified. In light of the possible relationship between taurine, muscle phenotype and atrophy and the modulating effects on the gCl, restCa, and MT, we decided to investigate the taurine content in the muscles of HU rats and the role of taurine in the prevention of muscle damage due to HU.

Methods

Treatment and animal care

All experiments were conducted in accordance with the Italian Guidelines for the use of laboratory animals, which conforms with the European Community Directive published in 1986 (86/609/EEC). Adult male Wistar rats (Charles River Laboratories, Italy) were used for the chronic and acute studies. The animals, weighing 300–350 g at the beginning of the experiments, were housed individually in appropriate cages in an environmentally controlled room. The animals were randomly assigned into four experimental groups: (1) a control group ($n = 15$) receiving a standard rodent diet (Provimi Kliba AG, Kaiseraugst, CH) (CTRL), (2) a ground-based group ($n = 14$) receiving 5% taurine supplemented diet (TAU), (3) a group ($n = 18$) of 14 day hindlimb-unloaded rats receiving a standard diet (HU), (4) a group ($n = 17$) of 14 day hindlimb-unloaded rats receiving the 5% taurine supplemented diet (HUTAU). The rats were fed with 100 g of food a day per kg of body weight, which corresponds to a maximum final taurine dose of 5 g/kg/day. All animals were given tap water ad libitum. To induce unloading, the animals were suspended by a shoelace linked at one extremity to the tail by sticking plaster and at the other extremity to a trolley that moves on horizontal rails at the top of the cage. The length of the shoelace was adjusted to allow the animal to move freely on its forelimbs, with the body inclined at 30° from the horizontal plane (Desaphy et al. 2001). At the end of treatment, all the rats were in good health. They were deeply anesthetized with urethane (1.2 g/kg i.p.) for surgery and killed thereafter by urethane overdose.

HPLC analysis for measuring taurine content

The trunk blood was collected in centrifuged tubes, rinsed with 10 µl of ethylenediaminotetraacetic acid (150 mM) and centrifuged at 600*g* for 10 min. The plasma was separated and stored at −20°C until it was used for taurine determination. The soleus and EDL muscles were weighed and homogenized with 10 ml of $HClO_4$ (0.4 N) per g of tissue. The homogenized muscles were buffered with 80 µl K_2CO_3 (5.5 g/10 ml) for each ml of $HClO_4$. The homogenates were centrifuged at 600*g* for 10 min at 4°C. The supernatants were stored at −80°C until the assay. Derivatization with ophthalaldehyde was performed as previously described and the samples were processed for HPLC taurine determination (De Luca et al. 2001). Taurine content was obtained as µmol/l from the homogenates prepared from the wet weighed muscle. Taurine content was normalized to muscle protein content (mg/100 ml) with a final concentration of µmol/mg as shown in Fig. 1. Because the soleus muscle undergoes severe atrophy that is characterized by protein degradation after HU, we theorized that it would be more accurate to normalize the taurine content to the protein quantity rather than to muscle weight. In this manner, we will elucidate the specific effect of HU on taurine content.

Immunohistochemistry and muscle fiber cross-sectional area

Expression of MHC isoforms was determined by immunofluorescence staining as described previously (Frigeri et al. 2001; Pierno et al. 2002; Desaphy et al. 2005). Briefly, soleus and EDL muscles were frozen in isopentane cooled in liquid nitrogen immediately after dissection. The sections were then incubated at 37°C for 1 h with monoclonal antibodies directed against adult MHC isoforms (Schiaffino et al. 1989) harvested from hybridoma cell lines (Developmental Hybridoma Studies Iowa, USA). The primary antibodies were detected by AlexaFluor 594-conjugated anti-mouse secondary antibodies (Invitrogen, CA, USA). The sections were mounted in a medium supplemented with DAPI and examined with a Leica DMRXA photomicroscope equipped for epifluorescence. Digital images were obtained with a Nikon DMX 1200 camera. For fiber quantification, the analysis was performed on 18 randomly chosen areas of three different sections of the same muscle. The number of examined animals was 3–4 for each treatment. To measure the cross-sectional area (CSA) of each fiber type, serial sections were in parallel stained with hematoxylin–eosin. The CSA was detected using NIS Elements software v.3.0 (Nikon, Tokyo, Japan) coupled with Adobe Photoshop CS4 software and the data were expressed in μm^2. Approximately 500 fibers per MHC class were measured.

Isolation of total RNA, reverse transcription and real-time PCR

For each muscle sample, total RNA was isolated with TRIzol (Invitrogen-Life Technologies) and quantified using a spectrophotometer (ND-1000 NanoDrop, Thermo

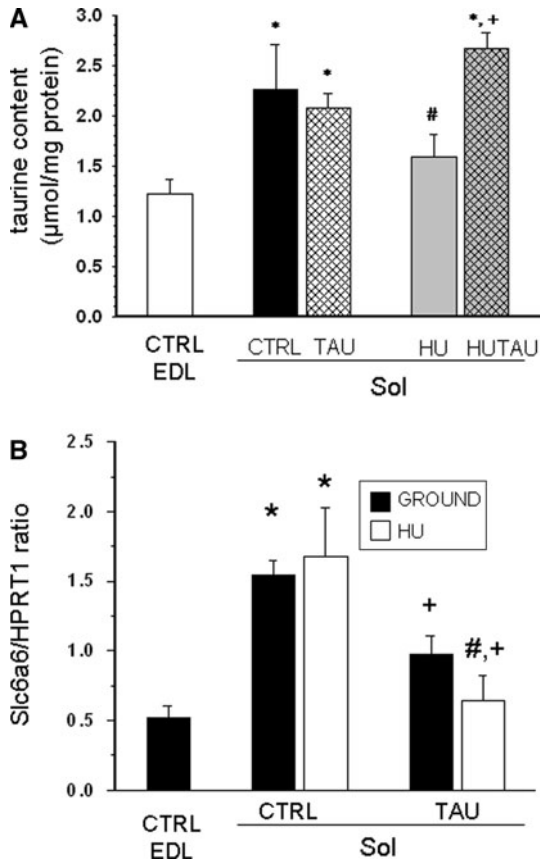

Fig. 1 Effects of hindlimb unloading and taurine supplementation on the levels of taurine in muscle and the TauT transporter (Slc6a6) mRNA expression. **a** Taurine content in extensor digitorum longus (*EDL*) of control rats and the soleus (*Sol*) muscles of control and hindlimb-unloaded rats fed with standard diet (CTRL and HU) or with diet supplemented with taurine (TAU and HUTAU). Each *bar* represents the mean ± SEM from 4 to 6 animals. Analysis of variance (ANOVA) showed significant differences in muscle taurine levels between the five experimental groups ($F = 4.5$, $P < 0.01$). *Symbols* indicate significant differences obtained by ad hoc Bonferroni's *t* test (at least $P < 0.05$) versus CTRL EDL (*), CTRL Sol (#), and HU Sol (+). **b** Levels of mRNA expression of Slc6a6, which encodes the Taurine transporter TauT, were determined using quantitative real time PCR. Each *bar* represents the mean ± SEM of TauT mRNA normalized to the housekeeping HPRT1 gene measured in the Sol and EDL muscles of 5 rats for each experimental group. The ANOVA test showed significant differences in TauT expression between the five experimental groups ($F = 7$, $P < 0.005$). *Symbols* indicate significant differences obtained by ad hoc Bonferroni's *t* test (at least $P < 0.05$) versus CTRL EDL (*), CTRL Sol (#), and HU Sol (+)

Scientific). To degrade any DNA contamination in each sample, 1 µg of the total RNA was incubated with 1 U of DNAse I (RNAse-free) (Ambion) at 37°C for 30 min and 75°C for 5 min. Total RNA (400 ng) was used for reverse transcription. Synthesis of cDNA was performed by using random hexamers (annealed 10 min, 25°C) and Superscript II reverse transcriptase (Invitrogen-Life Technologies) incubated at 42°C for 50 min. Real-time PCR was

Table 1 Genes used for the mRNA quantification

Gene	Protein	ID (ABI)	Amplicon pb
Fbxo32	Atrogin1	Rn00591730_m1	61
Hprt1	HPRT1	Rn01527840_m1	64
b2m	2βm	Rn00560865_m1	58
Slc6a6	TauT	Rn00567962_m1	140
Trim63	MURF1	Rn00590197_m1	56

performed in triplicate using the Applied Biosystems Real-time PCR 7500 Fast system and TaqMan® GenExpression Assays (Applied Biosystems) for each gene (Table 1). Each reaction was carried out as singleplex reaction. The setup of the reactions consisted of 8 ng of cDNA, 0.5 µl of each primer and probe set, 5 µl of TaqMan Fast Universal PCR master mix No AmpErase UNG (2×) (Applied Biosystems) and nucleotide-free H_2O for a final volume of 10 µl. The PCR conditions were: 95°C for 20 s; 95°C for 3 s; and 60°C for 30 s; steps 2 and 3 were repeated 45 times. The results were compared with a standard curve and normalized to the expression of the housekeeping gene HPRT1. As internal controls, the housekeeping genes HPRT1 and Beta-2 microglobulin (b2m) were analyzed. The analyzed genes are reported in Table 1.

Electrophysiological recordings by intracellular microelectrodes

The EDL and soleus muscles were dissected from deeply anesthetized rats and were immediately placed in a 25 ml muscle bathing chamber, maintained at 30°C. The muscles were perfused with normal or chloride-free physiological solutions (gassed with 95% O_2 and 5% CO_2; pH 7.2–7.3). As previously detailed (Bryant and Conte-Camerino 1991), the membrane electrical properties and the component conductances of sarcolemma were determined in a current-clamp mode by means of the standard two-intracellular-microelectrode technique. A hyperpolarizing square current pulse (100 ms duration) was passed through one electrode and the membrane voltage response was monitored at two distances from the current electrode (Pierno et al. 1998). According to the infinite linear cable theory we measured the experimental cable parameters, which include the space constant λ (logarithmic decay of the electrotonic potential with distance from the current electrode), the fiber input resistance, Rin (steady-state electrotonic potential divided by the current intensity) and the time constant τ (84% rise time of the electrotonic potential). The fiber diameter (d_{calc}) has been calculated from λ and Rin, and a constant value of 125Ω × cm was assumed for the myoplasmic resistivity on the basis of previous histological determinations (Bryant 1969; Pierno et al.

1998). From the above parameters, the membrane resistance (R_m) and the total membrane capacitance (C_m) were calculated. The current pulse generation, acquisition the voltage records and calculation of the fiber constants were done in real time under computer control as described elsewhere (Bryant and Conte-Camerino 1991). The reciprocal of R_m from each fiber in the normal physiological solution was assumed to be the total membrane conductance (g_m) and the same parameter measured in chloride-free solution was considered to be the potassium conductance (gK). The mean chloride conductance (gCl) was estimated as the mean g_m minus the mean gK (Bryant and Conte-Camerino 1991). For the in vitro evaluation of the acute effect of taurine on the gCl, the amino acid (30 and 60 mM) was dissolved in the physiological solution and was applied to the EDL and soleus muscle in the bathing chamber. The resting gCl was determined before and 30 min after the addition of taurine. Equimolar concentrations of sucrose or beta-alanine were used to examine any possible effects due to the osmotic change of the solution. The compounds at the two different doses tested (30 and 60 mM) did not mimic any of the effects observed with taurine at these concentrations on the gCl (De Luca et al. 2001; Conte Camerino et al. 1987, 1989). The mechanical threshold (MT) for contraction was determined in the muscle fibers using a computer-assisted two microelectrode point voltage clamp method in the presence of 3 μM tetrodotoxin, as described (De Luca et al. 2001; Pierno et al. 2002). The holding potential was set at −90 mV. Depolarizing current pulses of increasing duration (5–500 ms) were given repetitively (0.3 Hz rate), while the impaled fibers were viewed continuously with a stereomicroscope until visible contraction. The threshold membrane potential was read from a digital voltmeter. The mean threshold membrane potential V (mV) was plotted as a function of the pulse duration t (ms), and the relationship was fitted using the following equation: $V = [\text{H-Rexp}(t/\tau)]/[1 - \exp(t/\tau)]$, where H (mV) is the holding potential, R (mV) is the rheobase voltage, and τ (ms) is the time constant to reach R. The MT values were expressed as the fitted R parameter along with the standard error that was determined from the variance–covariance matrix in the no-linear squares fitting algorithm.

Fura-2 microfluorescent analysis

The resting cytosolic Ca^{2+} concentration (restCa) was determined in freshly, mechanically dissected muscle fibers using a QuantiCell 900 fluorescence imaging system (Visitech International, Sunderland, UK), as previously described (Fraysse et al. 2003). Briefly, small bundles of 5–10 fibers were dissected tendon to tendon, from the soleus and EDL muscles. The muscle fibers were incubated with the fluorescent Ca^{2+} probe Fura-2 for 60–90 min at 30°C in a physiological solution (NP solution containing 148 mM NaCl, 4.5 mM KCl, 2.5 mM $CaCl_2$, 1 mM $MgCl_2$, 12 mM $NaHCO_3$, 0.44 mM NaH_2PO_4, 5.5 mM glucose; pH 7.3–7.4) supplemented with 5 μM of acetoxymethyl ester of the dye mixed to 10% (v/v) with pluronic F-127 (Molecular Probes, Leiden, The Netherlands). After incubation, the cells were washed with NP solution and mounted in a modified RC-27NE recording chamber (Warner Instruments, Hamden, CT). The tendons of the bundles were attached by hair loops, with one extremity to a fixed tube, and the other to a mobile one. The chamber was placed on the stage of an inverted Eclipse TE300 microscope equipped with a 40× plan-fluor objective (Nikon, Tokyo, Japan) and was continuously perfused with NP solution at a constant rate of ~4 ml/min (Warner Instruments). The fiber integrity was verified by assessing the visible contractile activity under 400× magnification in response to a depolarizing solution containing 100 mM K^+. The mean sarcomere length was adjusted to ~2.5 μm. The mean resting background-corrected ratio (340/380 nm) values were determined for each fiber of the bundle by manually demarcating fiber boundaries using the QC2000 software. This fluorescence ratio was converted offline to restCa by using the calibration parameters determined in each muscle, and the equation $\text{restCa} = (R - R_{min})/(R_{max} - R)K_D\beta$, where R is the 340–380 nm fluorescence ratio; K_D is the affinity constant of Fura-2 for Ca^{2+} given by the manufacturer (i.e. 145 nM, Molecular Probes), and β, R_{min}, and R_{max} are the calibration parameters determined in ionomycin-permeabilized fibers bathed in NP solution for the calculation of R_{max} or in Ca^{2+}-free solution for the calculation of R_{min} (Grynkiewicz et al. 1985). The β value was calculated as the ratio of fluorescence intensities emitted by the fibers excited at 380 nm in Ca^{2+}-free and NP solutions. The calibration parameters were measured for every muscle type in each experimental condition (Gailly et al. 1993; Fraysse et al. 2003). The manganese quench technique was used to estimate the sarcolemmal permeability to divalent cations (Fraysse et al. 2003). Mn^{2+} enters cells via the same routes as Ca^{2+} and accumulates inside over time because it is poorly accepted by the cellular transport systems. As Mn^{2+} quenches the fluorescence of Fura-2, the reduction of the intensity of Fura-2 fluorescence can be used as an indicator of the time integral of Mn^{2+} influx. Muscle preparations were first perfused for 2 min with NP solution containing 0.5 mM Mn^{2+} as a surrogate of Ca^{2+} (quenching solution). Then, the quenching solution supplemented with 30 mM taurine was applied to the muscle fibers for 2–4 min. During the whole quenching protocol, the fluorescence of Fura-2 excited at 360 nm was acquired at 1 Hz. The quench rates were estimated using linear regression analysis of the fluorescent signal and expressed as the decline per minute of the initial fluorescence intensity.

Statistical analysis

All data are expressed as mean ± SEM. The estimates for SEM and number of fibers (n) of gCl were obtained from the variance of gm and gK, assuming no covariance, and from the number of fibers sampled for gm and gK, respectively (Bryant and Conte-Camerino 1991). The analysis of variance (ANOVA) followed by Bonferroni's t test was used to evaluate statistical differences between the treated and control groups. A comparison of means from each treated rat and the related control group was evaluated by the unpaired Student's t test.

Results

Taurine content in fast- and slow-twitch skeletal muscle of control, HU, and taurine-treated HU rats

As already shown by others (Dawson et al. 2002), we found significant differences in the taurine content between the fast-twitch and the slow-twitch rat skeletal muscles. The taurine content was almost twofold higher in the slow soleus muscle than in the fast EDL muscle, with values of 2.26 ± 0.45 µmol/mg ($n = 5$) and 1.22 ± 0.14 µmol/mg ($n = 4$), respectively. After 14 days of HU, the taurine content in the soleus muscle was significantly reduced to a value similar to that of the EDL muscle (Fig. 1a). The plasma taurine content was found to be higher in HU rats compared to control animals, with values of 533 ± 170 µmol/l ($n = 7$) vs. 322 ± 58 µmol/l ($n = 5$), respectively. This was probably caused by the loss of taurine in the muscles or possibly other tissues. Dietary taurine supplementation significantly increased plasma taurine content in both the control and HU animals, with values of 1,330 ± 442 µmol/l ($n = 6$, $P < 0.05$ by ANOVA/Bonferroni) and 2,435 ± 531 µmol/l ($n = 6$, $P < 0.005$ by ANOVA/Bonferroni), respectively. This increase had no effect on the concentration of taurine in the soleus muscle of the control animals, but it prevented the drop in taurine content in the HU soleus muscle. Dietary taurine supplementation significantly increased the amount of taurine in the soleus muscle with respect to the untreated HU soleus muscle (Fig. 1a).

Effects of taurine treatment on phenotype transition and muscle atrophy of HU rats

As previously described (Pierno et al. 2002) 85% of the fibers of the soleus muscle in control rats express the slow-twitch, type I myosin heavy chain (MHC-I) isoform, and the remaining fibers express the fast-twitch MHC-IIa isoform. It is well known that after HU, the expression of the fast MHC isoforms significantly increases in rat soleus muscle as a feature of the slow-to-fast transition (Talmadge et al. 1996; Stevens et al. 1999; Pierno et al. 2002; Desaphy et al. 2005). In the present study, immunohistochemical analysis showed a significant increase of fast-twitch MHC-positive fibers including the pure MHC-IIa and hybrid type MHC-I/IIa, in soleus muscles from 15% of the control to 33% after 14 days of HU (Fig. 2a, b). We have previously demonstrated that hybrid types MHC-I/IIa are typically expressed during HU (Desaphy et al. 2005). In addition, the slow-twitch type I MHC-positive fibers were reduced from 84 to 67% (Fig. 2b). Supplementation with taurine had no effect on the fast or slow MHC-positive fiber distribution in control rats, but it significantly prevented the changes in MHC expression in the soleus muscle of HU rats (24% of fast MHC-positive fibers and 76% of slow MHC positive fibers with a reduction of both pure IIa and hybrid I/IIa MHC fibers), suggesting that taurine supplementation partially prevents the HU-induced phenotype transition (Fig. 2a, b). In the EDL muscle the number of MHC I and II fibers were almost unchanged (Fig. 4a). Another important hallmark of HU is the atrophy that progressively develops in disused soleus muscle (Pierno et al. 2002). In this study, we evaluated muscle atrophy by measuring the soleus muscle-to-body weight ratio and calculating the soleus muscle fiber CSA. The muscle-to-body weight ratio was significantly reduced in the HU rats (Fig. 3a). Interestingly, the CSA was significantly reduced in the type I and in type II fibers of soleus muscle (Fig. 3b–d). No beneficial effect of taurine supplementation was found on these parameters in the soleus muscle of HU rats. Indeed the CSA was still lower than the control in the type I and type II fibers (Fig. 3b–d). The CSA was not changed in the taurine-treated soleus muscle (Fig. 3b–d). In the EDL muscle, we did not observe any modification of the CSA either in the fast or in the slow fibers (Fig. 4b). In Fig. 2a representative muscle sections showing the reduction of the CSA in HU and HU treated soleus muscle and the modification of fast MHC by the anti-fast antibody in the different experimental conditions are shown. These data are in accordance with the significant reduction in fiber diameter measured from cable parameters in the current clamp mode by the two microelectrode technique in HU rat soleus muscle. Indeed fiber diameter was 62 ± 1.6 µm ($n = 50$) in the control soleus muscle and 43 ± 0.8 µm ($n = 50$, $F = 74$, $P < 0.001$ by ANOVA/Bonferroni) in the HU soleus muscle. This reduction was not restored in the taurine-treated HU rat soleus muscle (39 ± 1.0 µm, $n = 49$, $P < 0.001$ by ANOVA/Bonferroni).

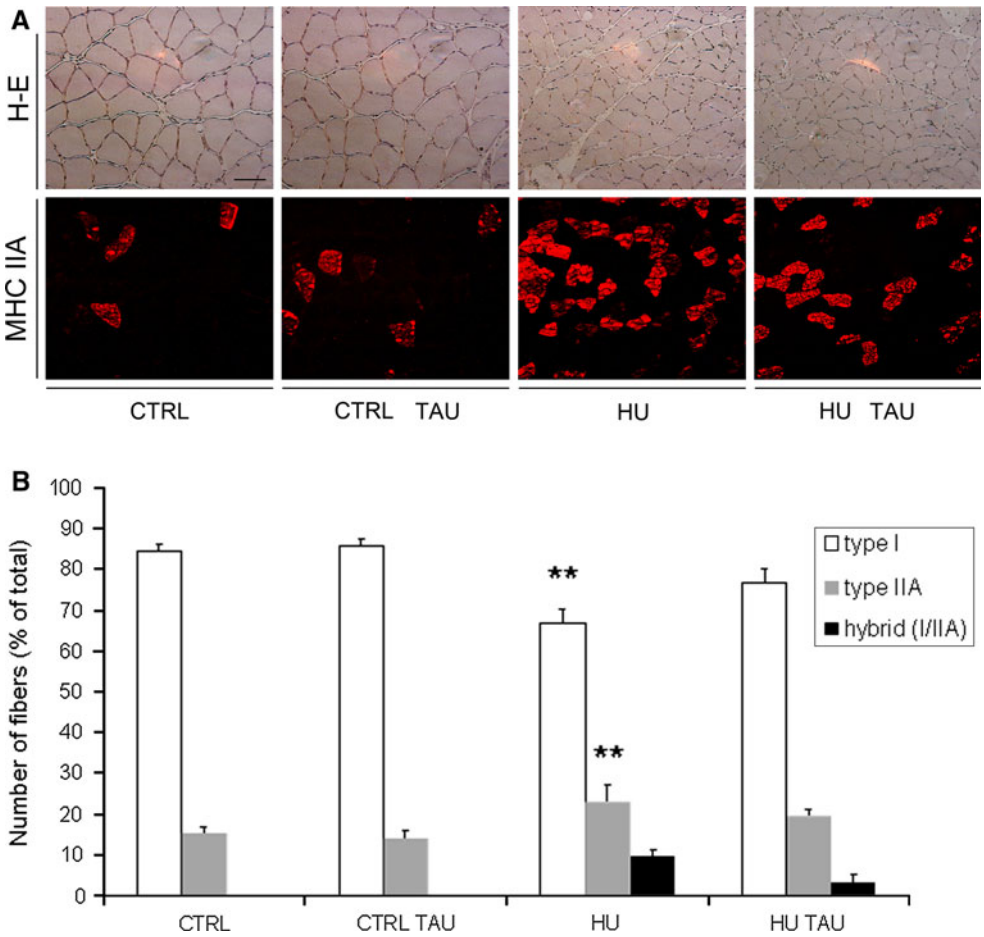

Fig. 2 Effects of hindlimb unloading and taurine supplementation on MHC isoform distribution in soleus muscles of control rats (CTRL), taurine-treated rats (CTRL TAU), hindlimb-unloaded rats (*HU*) and hindlimb-unloaded rats treated with taurine (HU TAU). **a** Representative examples of soleus muscle sections stained with hematoxylin–eosin (H–E) or with antibody against type IIA myosin heavy chain. *Scale bar* 50 μm. **b** MHC distribution in soleus muscle of CTRL, CTRL TAU, HU and HU TAU. The percentage of MHC-I positive fibers and MHC-IIa positive fibers and hybrid fibers positive to type I and type IIA MHC was determined by densitometric analysis. **Significantly different with respect to CTRL (one-way ANOVA followed by Bonferroni's test, $F = 10$, $P < 0.02$ or less)

Effects of taurine treatment on gene expression in the skeletal muscle of control and HU rats

In the present study, we measured the mRNA amount of the taurine transporter TauT in the soleus and EDL muscles of CTRL, HU, and taurine treated rats using quantitative real time PCR. The EDL muscle in the control rats expresses about one-third of TauT mRNA compared to the soleus muscle of the control rats (Fig. 1b). After 14 days of HU, the TauT mRNA expression did not change with respect to the relative control. Interestingly, taurine treatment significantly reduced TauT expression both in the soleus muscle of control rats and in the soleus of HU rats, this is likely due to a negative feedback of high taurine levels on TauT expression (Tappaz 2004). Also, in EDL muscle, a reduction of TauT was found in the taurine-treated HU rats with respect to the control (not shown). As expected, we found an increase of atrogin in the soleus muscle of HU rats, which was slightly but not significantly reduced by taurine treatment (Fig. 5a). We also evaluate the expression of another atrophy-related gene, MURF-1. As expected, MURF-1 expression was increased in the HU rats, but surprisingly it was significantly restored by taurine treatment (Fig. 5b).

Effects of taurine treatment on skeletal muscle chloride conductance modified by HU in rats

In agreement with previous findings (Pierno et al. 2002, 2007) we found a lower value of gCl in the slow-twitch soleus muscle with respect to the fast EDL muscle, with values of $1{,}707 \pm 37$ and $2{,}727 \pm 80$ μS/cm^2, respectively. As previously demonstrated, the resting gCl increased by 30% in the HU soleus muscles toward that of the fast EDL, which was in accordance with the partial transition of the soleus muscle phenotype (Fig. 6a). Taurine supplementation did not change the gCl in the control soleus muscle, but it completely prevented the increase in gCl in the soleus muscle of HU rats (Fig. 6a). We also tested the effect of acute application of taurine on chloride conductance in vitro. We have previously described that in vitro application of taurine to rat EDL muscle significantly increased resting gCl in a dose-dependent manner (Conte Camerino et al. 1987). Accordingly, we found a 40% increase of gCl in the EDL muscle when 30 mM taurine was applied. Here, we demonstrated that the gCl sensitivity to taurine is lower in the soleus compared to the EDL muscle fibers, and this is probably because of the higher taurine content in the slow-twitch muscle. Indeed, in vitro

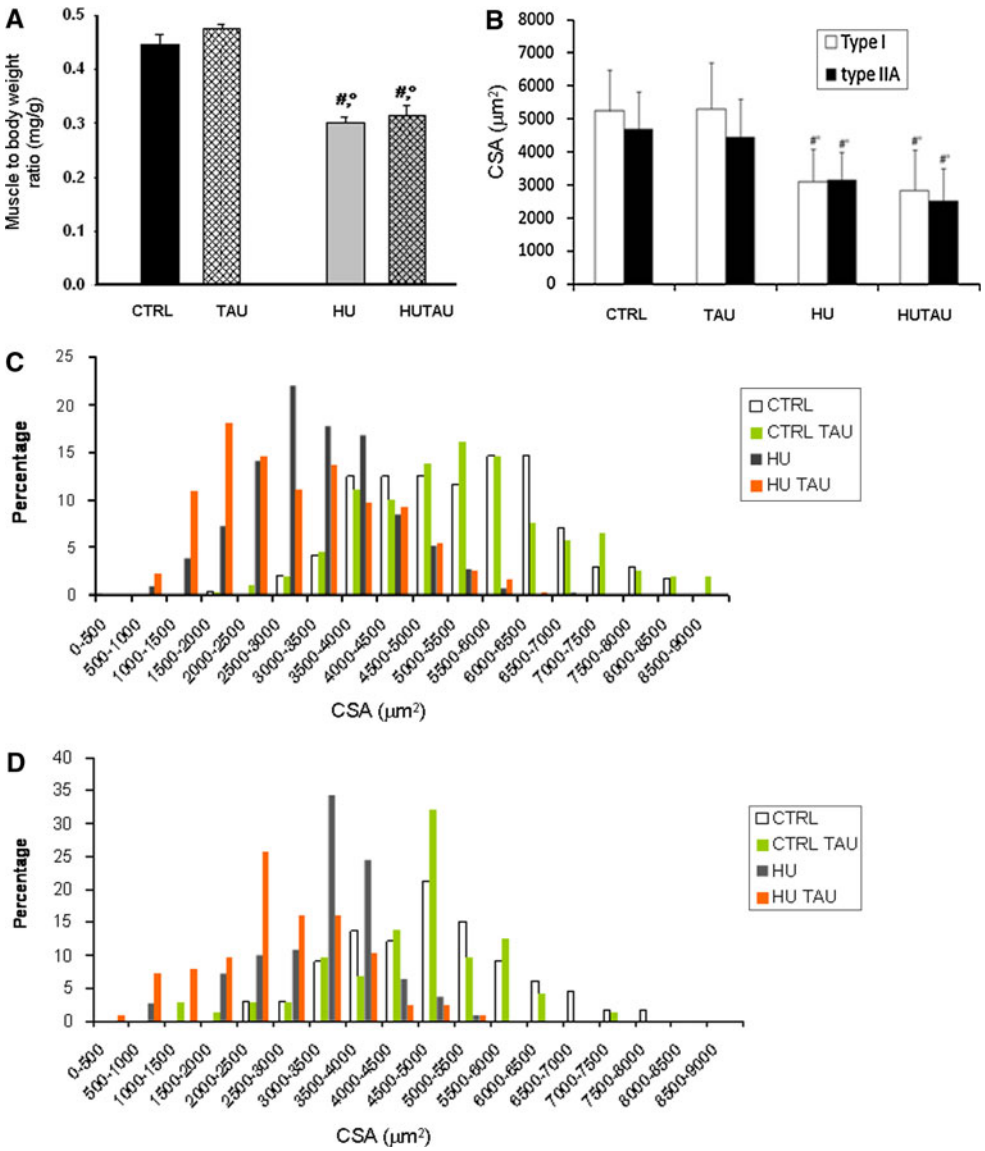

Fig. 3 Soleus muscle atrophy after hindlimb unloading and taurine treatment. **a** *Bars* indicate the mean soleus muscle-to-body weight ratio ±SEM from 5 to 6 rats in each experimental condition. Analysis of variance showed significant differences between the groups ($F = 31.7$, $P < 0.001$). Bonferroni's t test indicated significant differences (at least $P < 0.05$) versus CTRL (#) and TAU (°). **b** *Bars* show the mean cross-sectional area (CSA) ± SEM measured in fibers stained for type I or type IIA MHC. ANOVA indicates significant differences between the groups. Significant difference versus #CTRL and *TAU was found following ad hoc Bonferroni's test ($P < 0.05$ or less). **c**, **d** Fiber distribution as a function of CSA in type I and type II MHC-positive fibers of soleus muscle in the four experimental conditions

application of 30 and 60 mM taurine increased gCl in the soleus muscle by only 3 and 22%, respectively. After HU, the gCl sensitivity to taurine was increased in the soleus muscle, which is in accordance with the fiber type transition and the decreased taurine content in the HU soleus muscle, showing a 38% increase in the presence of 30 mM taurine. Long-term supplementation with taurine prevented the change of gCl sensitivity to taurine in vitro application in the soleus muscle of HU rats, which is consistent with the prevention of the drop in taurine content. Indeed, the increase in gCl was 14 and 20%, in the presence of 30 and 60 mM taurine, respectively (Fig. 6b). It should be noted that the apparent discrepancy between the gCl increase induced by taurine in vitro and the gCl increase that occurs in parallel to a reduction in the taurine content induced in vivo by HU most likely reflects a mechanistic difference between acute and long-term effects. While the acute effect is likely due to a rapid biochemical modulation of the gCl, the long-term effect may result secondarily to the modulation of the muscle phenotype (Conte Camerino et al. 1989).

Effects of taurine treatment on the resting cytosolic calcium concentration and calcium homeostasis in the skeletal muscle of HU rats

In the control animals, the resting cytosolic calcium concentration was 1.6-fold higher in the soleus with respect to the EDL muscle (Fig. 7a). After HU, cytosolic calcium in soleus muscle was significantly reduced toward that of the EDL, as previously shown (Fraysse et al. 2003). In the taurine-treated HU rats the reduction of resting [Ca^{2+}] in the soleus muscle fibers was fully prevented (Fig. 7a). This effect was exclusively observed in HU rats administered

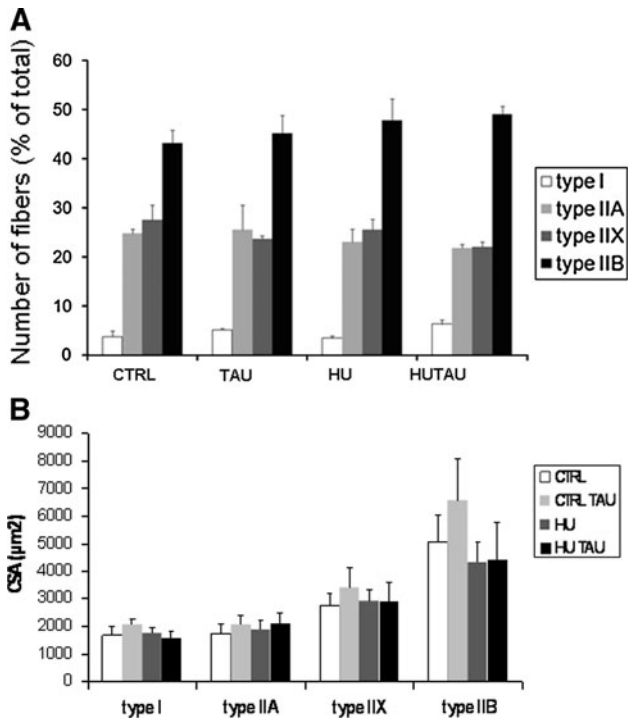

Fig. 4 Effects of hindlimb unloading and taurine supplementation on MHC isoform distribution and fiber cross-sectional area in the EDL muscle of control rats (CTRL), taurine-treated rats (CTRL TAU), hindlimb-unloaded rats (*HU*) and hindlimb-unloaded rats treated with taurine (HU TAU). **a** The percentage of MHC-I, MHC-IIA, MHC IIX and MHCIIB positive fibers was determined by densitometric analysis in the different experimental situations. **b** CSA of type I, IIA, IIX, and IIB fibers was determined in EDL muscle in the different experimental situations. No significant differences were found

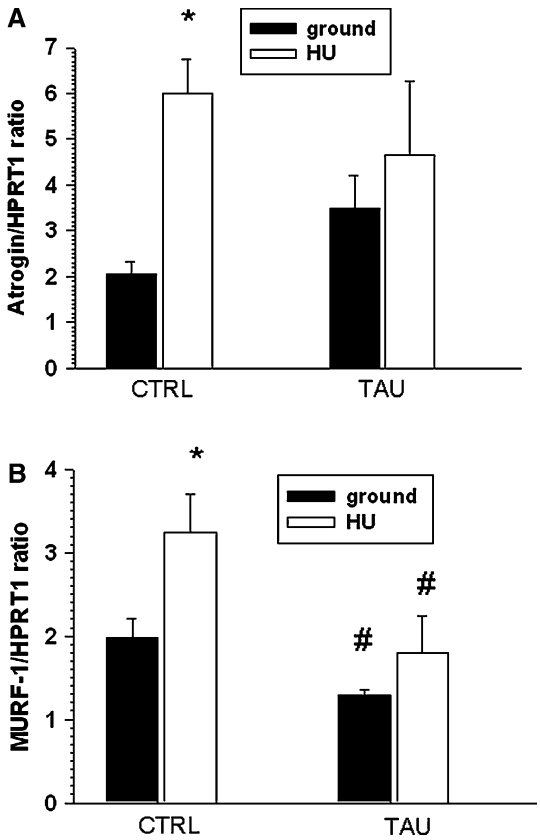

Fig. 5 Effects of HU and taurine treatment on mRNA expression of atrogin-1 (**a**) and MURF-1 (**b**) determined by real time PCR. Each *bar* represents the mean value ± SEM of atrogene mRNA normalized to the housekeeping HPRT1 gene measured in soleus muscles of five rats in each experimental condition: control (CTRL), hindlimb-unloaded (HU), ground-based treated with taurine (TAU), and HU treated with taurine (HUTAU). Statistical analysis was performed using ANOVA (atrogin-1: $F = 2.96$, ns; MuRF-1: $F = 5.89$, $P < 0.01$) followed by ad hoc Bonferroni's t test ($^{*}P < 0.05$ or less vs. CTRL; $^{\#}P < 0.02$ or less vs. HU)

with taurine, since the restCa level in the soleus muscle fibers was not modified in the taurine-treated control animals (Fig. 7a). As previously demonstrated (Fraysse et al. 2003) by using the Mn^{2+} quenching technique, the sarcolemmal permeability to calcium was decreased in HU soleus muscle with respect to control soleus muscle to values similar to those found in EDL. Specifically, the mean quench rate was 4.3 ± 0.2%/min ($n = 44$) and 3.2 ± 0.2%/min ($n = 49$) in the soleus and HU soleus muscle, respectively. Interestingly, in vivo treatment with taurine significantly prevented the reduction of the mean quench rate in HU rats (4.8 ± 0.32%/min, $n = 88$), showing an amino acid-induced restoration of sarcolemmal permeability to calcium. The mean quench rate of 4.34 ± 0.33%/min ($n = 54$) was not modified in the taurine-treated control group. The ANOVA statistical analysis showed significant differences among the groups ($F = 4.9$; $P < 0.005$); the Bonferroni t test showed significant differences between the HU and CTRL groups ($P < 0.05$) and between the HUTAU and HU groups ($P < 0.001$). In vitro experiments demonstrated that the application of 30 mM taurine to HU soleus muscle fibers increased sarcolemma permeability from a quench rate value of 3.4 ± 0.2%/min ($n = 10$) to 4.9 ± 0.3%/min ($n = 10$) ($P < 0.001$ by Student's t test). These results demonstrate a direct effect of taurine in the stimulation of calcium influx (Fig. 7b), whereas the quench rate values did not change in the control rats (not shown).

Effects of taurine treatment on the mechanical threshold for contraction in the skeletal muscle of HU rats

The mechanical threshold (MT) is an index of excitation–contraction coupling (De Luca et al. 2001). The threshold potential needed to elicit contraction is determined by applying a current pulse for different durations (5–500 ms) of stimulation. The rheobase voltage (R, mV), is the most negative voltage able to elicit contraction, and is calculated from the fit of the strength-duration relationship. As

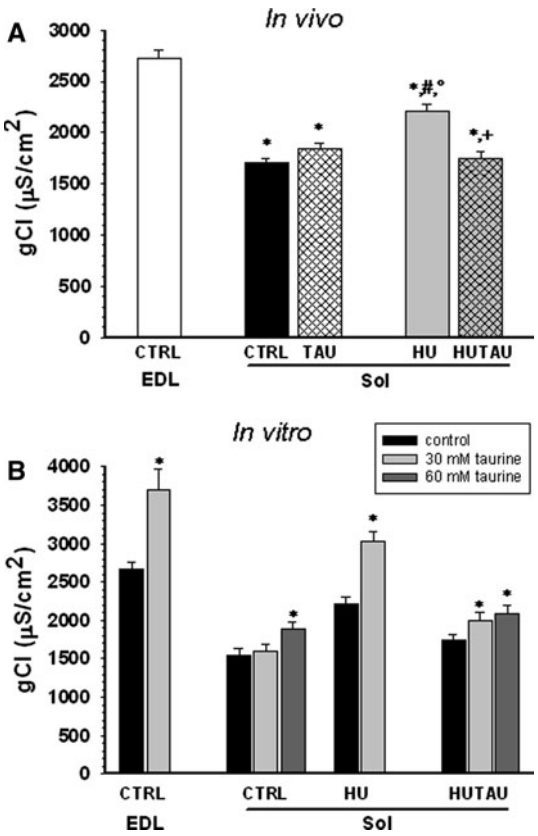

Fig. 6 Effects of taurine chronic administration (in vivo) and acute application (in vitro) on resting chloride conductance (gCl) of HU rat skeletal muscle. **a** Resting gCl measured in the extensor digitorum longus (*EDL*) of control rats and soleus (*Sol*) muscles of control and hindlimb-unloaded rats fed with a standard diet (CTRL and HU) or with a diet supplemented with taurine (TAU and HUTAU). Each *bar* represents the mean ± SEM from 40 to 52 fibers of 3–5 animals. Analysis of variance indicates significant differences in resting gCl between the five experimental groups ($F = 41$, $P < 0.001$). *Symbols* indicate significant differences obtained by ad hoc Bonferroni's *t* test (at least $P < 0.001$) versus CTRL EDL (*), CTRL Sol (#), TAU (°), and HU (+). **b** Effects of in vitro application of 30 and 60 mM taurine on the resting gCl of control rat EDL muscles and Sol muscles of CTRL, HU, and HUTAU rats. Each *bar* represents the mean gCl ± SEM from 12 to 50 fibers of 2–4 muscle preparations. *Symbol* indicates at least $P < 0.05$ with respect to the gCl measured in the absence of taurine (unpaired Student's *t* test)

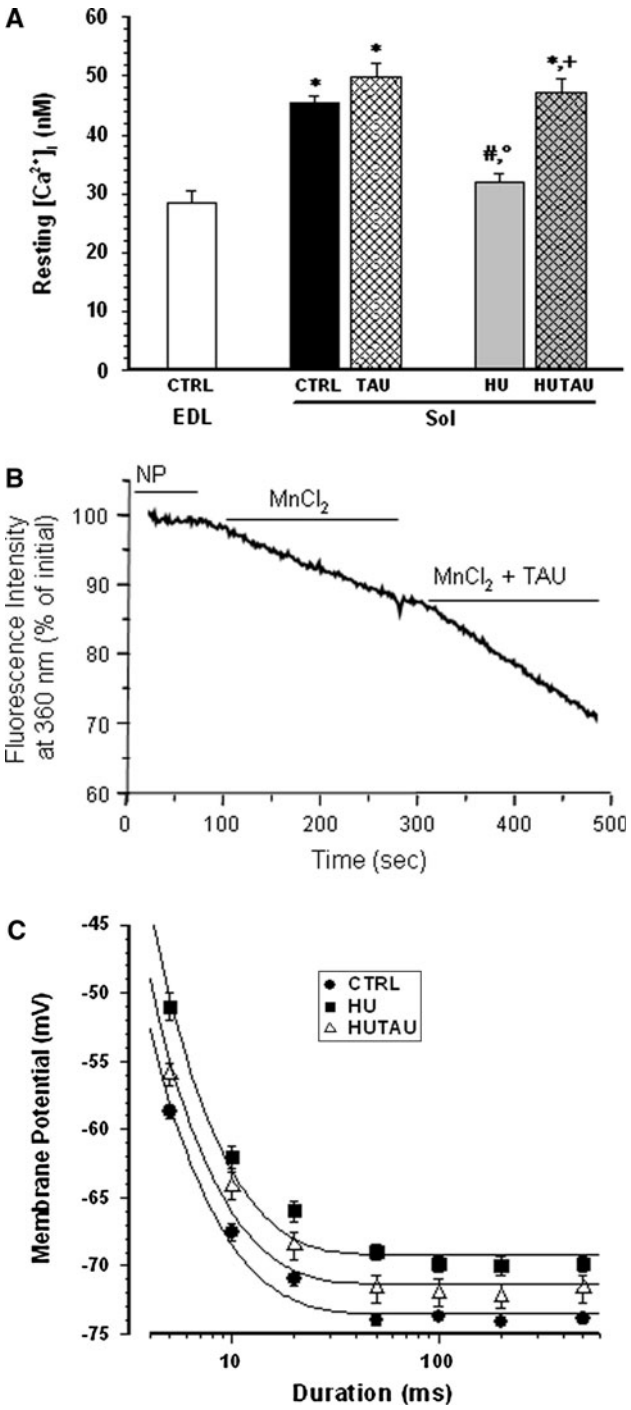

already demonstrated (Pierno et al. 2002), the *R* voltage was more negative in the soleus with respect to the EDL muscle (−73.3 ± 0.8 vs. −65.5 ± 0.9 mV, $P < 0.001$ by Student's *t* test) but was shifted toward a less negative voltage (−69.5 ± 0.7 mV vs. control Sol, $P < 0.001$) in the HU soleus muscle, as expected from the fiber type transition. Taurine supplementation did not modify the *R* voltage in the soleus muscle of control rats (not shown), but it partially prevented the *R* shift in the soleus muscle of HU rats (−71.7 ± 0.6 mV), making this value similar to that of the control Sol muscle ($t = 1.62$, ns) (Fig. 7c).

Discussion

The role of taurine in fast and slow-twitch muscle function

Taurine uptake into skeletal muscles is notoriously dependent on the activity of the Na^+/Cl^--dependent taurine transporter TauT. The activity and expression of this carrier are higher in slow- compared to fast-twitch muscles,

◀ **Fig. 7** Effect of hindlimb unloading (HU) and taurine supplementation on calcium homeostasis in rat skeletal muscle. **a** Resting cytosolic calcium concentration (restCa) measured in the extensor digitorum longus (*EDL*) of control rats and soleus (*Sol*) muscles of control and hindlimb-unloaded rats fed with standard diet (CTRL and HU) or with diet supplemented with taurine (TAU and HUTAU). Each *bar* represents the mean ± SEM from 40 to 76 fibers of 3–7 animals. Analysis of variance indicates significant differences in resting gCl between the five experimental groups ($F = 25.3$, $P < 0.001$). *Symbols* indicate significant differences obtained by ad hoc Bonferroni's *t* test (at least $P < 0.001$) versus CTRL EDL (*), CTRL Sol (#), TAU (°), and HU (+). **b** Typical recordings illustrating the effects of taurine on Fura-2 fluorescence quenching associated with Mn^{2+} ($MnCl_2$) influx in Sol muscle fiber of HU rats. The decline of Fura-2 fluorescence is expressed as a percentage per minute of initial fluorescence intensity. The quench rates were determined using linear regression analysis, before and after application of taurine, as reported in the text. *NP* normal physiological solution. **c** Strength-duration curves for the threshold potential of mechanical activation in Sol muscle fibers from CTRL ($n = 4$), HU ($n = 5$), and HUTAU ($n = 6$) rats. Each point is the mean value ± SEM of the threshold potential (in mV) recorded at each pulse duration from 27 to 98 fibers. The equation used for fitting the relationships is reported in the "Methods". The fitting parameters are reported in the text

which contributes to the difference in taurine content between the muscle types (Kim et al. 1986; Iwata et al. 1986). The concentration of taurine is twofold higher in soleus compared to EDL muscle. However, the physiological relevance of the proper concentration of taurine critical for phenotype determination is unknown. Various hypothesis can be formulated on the basis of the proposed role of taurine in skeletal muscle, such as protection against oxidative stress, calcium homeostasis regulation, or cell osmoregulation. A large amount of taurine was correlated to the oxidative capacity of the muscles, suggesting a specific role for the amino acid in muscle metabolism (Yoshioka et al. 2002). Because taurine displays antioxidant activity and is present in mitochondria, it may be hypothesized that the amino acid helps oxidative muscles, that are rich of mitochondria, to protect themselves from free radical production. In addition, because taurine modulates muscle calcium homeostasis by acting on sarcolemma ion channels, sarcoplasmic reticulum (Satoh and Sperelakis 1998; Bakker and Berg 2002) and mitochondria (El Idrissi 2008) the amino acid may play a critical role in phenotype-specific, Ca^{2+}-dependent cellular functions.

Taurine content modification in slow-twitch soleus muscle after hindlimb unloading

Here we found that the taurine content was markedly decreased in HU soleus muscle, in parallel with the transition toward a faster phenotype. However, in this situation TauT expression was not reduced toward the values found in the EDL muscle, suggesting that the intracellular reduction of taurine is not attributable to a decreased expression of TauT. Also the positive effect of taurine supplementation on HU-Sol muscle content observed in this study suggests that an efficient TauT-transport activity is maintained during HU. In addition, taurine content has been shown to be reduced in soleus muscle chronically stimulated at a high frequency for 14 days without a modification in taurine uptake (Kim et al. 1986). Thus, we hypothesize that the reduction of intracellular taurine content during HU is not due to a decreased influx, but it is likely due to taurine efflux. Accordingly, taurine depletion was accompanied by an increase in its blood concentration in HU rats, which is in agreement with the loss from soleus muscle and probably from other tissues. Indeed, a reduction of taurine level was also observed in the sensorimotor cortex of HU rats (Canu et al. 2006). A possible explanation might be that taurine leakage compensates for intracellular osmolarity changes, which likely occur due to muscle protein degradation. Taurine efflux is generally regulated by osmolarity. Although we have no direct measure of the osmolarity change in HU muscles, it is worth noting that proteolysis is known to occur during HU-induced atrophy (Fujino et al. 2009; Ferreira et al. 2009) and that the degradation of proteins into amino acids and other macromolecules (i.e. glycogen, and fatty acids) increases the number of osmotically active compounds, contributing to the increase of intracellular osmolarity (Lang 2007). In this state, cells may respond by rapid swelling followed by an active extrusion of intracellular osmotically active solutes including taurine (Pasantes-Morales et al. 1990). Taurine loss from muscle has been observed during endurance exercise during which the effects on intracellular osmolality are acute and due to the accumulation of lactate and the breakdown of phosphocreatine (Cuisinier et al. 2002). Interestingly, there are some studies reporting lactate production during muscle disuse atrophy which justifies taurine escape in this condition as well (Ojala et al. 2001; Stein and Wade 2005; Grichko et al. 2000).

Effects of taurine supplementation in soleus muscle modified by hindlimb unloading

Taurine supplementation in HU rats maintained the taurine content of soleus muscle and prevented partial phenotypic changes, including MHC expression patterns, the gCl, and calcium ions. These effects were obtained with a high daily dose of taurine, but we did not observe any side effects in the treated animals. It should be mentioned that taurine competes with beta-alanine for TauT transport, which may result in reduction of carnosine production. Nevertheless, we found no variation in the EDL muscle function of treated rats, although the fast-twitch muscles are the more sensitive to carnosine homeostasis (Baguet et al. 2011).

Taurine is known to modulate calcium homeostasis in skeletal muscle (Huxtable 1992) and the Ca^{2+}-dependent cellular functions. For this reason the amino acid may play a critical role in phenotype modulation. Calcium signalling through calcineurin is a main regulatory pathway of type I fiber-selective gene expression (Lin et al. 2002). We have previously shown that during HU, the restCa is modified according to the change of phenotype in soleus muscle (Fraysse et al. 2003). Thus, a decrease in taurine may contribute to the reduction of cytosolic calcium, which in turn may remove the inhibitory effect of PKC on the resting gCl in slow-twitch muscle fibers (Pierno et al. 2007). Accordingly, taurine supplementation in HU rats allowed for the maintenance of high taurine content and calcium concentration and a low gCl in the soleus muscle. Quite surprisingly, these results do not match with those obtained in previous studies investigating other physiopathological conditions. For instance, we previously demonstrated that sarcopenia in aged rats was accompanied by a decrease in taurine content, an increase of restCa, and a decrease in gCl due to an increased PKC activity (Pierno et al. 1998; Fraysse et al. 2006). In addition, taurine depletion obtained in vivo by the administration of guanidinoethan sulfonate (GES), an inhibitor of TauT, markedly reduced the gCl and modified the excitation-contraction coupling mechanism in EDL muscle (Conte Camerino et al. 2004). It should be underlined, however, that all these effects were observed only in the fast-twitch EDL muscle, a muscle not affected by the HU condition (Pierno et al. 2002). This suggests that the effects of taurine depletion on muscle function strictly depend on the muscle phenotype. It is also possible that the effects of taurine depletion are dose-dependent, because the reduction of intracellular taurine levels due to GES administration is likely greater than that observed in HU muscles (>50 vs. ~40%, respectively). Similarly, a great reduction of muscle taurine content >98% in TauT−/− knockout mice induces a severe muscle impairment. Finally, while taurine intake is completely inhibited in the presence of GES or by TauT gene deletion, the basic mechanism of taurine reduction during HU may be different because the amino acid likely circulates from the muscle to the blood. Besides the modulation of calcium homeostasis, another mechanism possibly involved in the effect of taurine supplementation on muscle phenotype may be the protection against oxidative stress. Production of free radicals has been consistently reported in the muscles of HU rodents, and we recently demonstrated that in vivo treatment of HU mice with the antioxidant trolox partially prevented the shift of the muscle phenotype, maintaining the distribution of MHC isoforms and a low gCl in HU soleus muscle (Desaphy et al. 2010). By modulating the rate of ROS production in the mitochondria (El-Idrissi 2008), taurine supplementation may limit oxidative stress in HU muscles thereby counteracting the phenotype transition. In addition to its effect on muscle phenotype determination, the reduction of taurine content in skeletal muscles may have other important functional consequences. Indeed, taurine depletion obtained in vivo by GES administration induces the loss of muscle strength in the fast-twitch EDL of mice (Hamilton et al. 2006). It is thus possible that taurine depletion in HU soleus muscle may contribute to the reduction of muscle strength, which typically occurs either during HU (Gardetto et al. 1989) or in other pathological conditions, such as the muscular dystrophy of mdx mice in which taurine treatment increases the intracellular taurine content and ameliorates muscle strength and contractility (Cozzoli et al. 2011). Although taurine supplementation restored many functions, it had little effect on muscle atrophy, which is a severe condition occurring in various muscle diseases (Murton et al. 2008). Nevertheless, we discovered that although it did not prevent the reduction of muscle-to-body weight ratio and of the fiber CSA, taurine ameliorated the gene expression level of atrogin-1 and MURF-1, two key enzymes involved in HU-induced

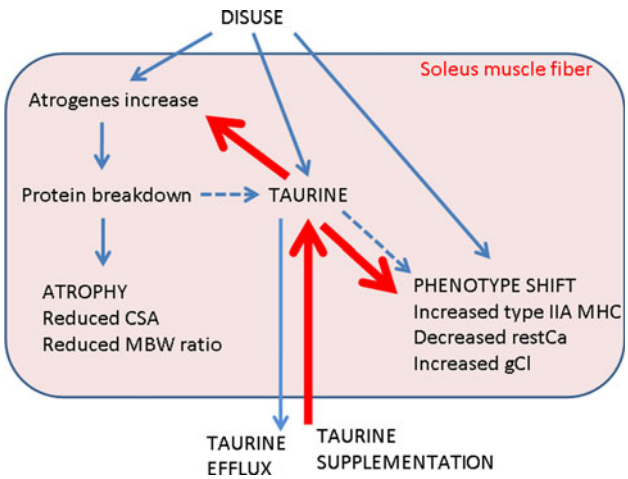

Fig. 8 The picture illustrates the soleus muscle impairment induced by HU. *Plain thin arrows* indicate the demonstrated effects of muscle disuse. Muscle disuse results in up-regulation of atrogenes that promote protein breakdown, resulting in muscle atrophy that is characterized by a reduction of cross-sectional area (CSA) and muscle-to-body weight (MBW) ratio. In parallel, muscle disuse induces a slow-to-fast shift of the phenotype, characterized by increased expression of type IIA myosin heavy chain (MHC), decreased resting calcium concentration (restCa), and increased chloride conductance (gCl). A reduction of taurine content is also observed, which most likely results from taurine efflux out of the muscle fiber. *Dashed thin arrows* show the possible mechanisms, including the possible role of protein breakdown in inducing taurine release, and the possible contribution of taurine content reduction in the induction of the phenotype shift. *Thick arrows* indicate that taurine supplementation restores taurine content thereby counteracting the phenotype shift. In addition taurine supplementation was shown to reduce the expression of atrogenes

atrophy (Bodine et al. 2001). Such an effect suggests that a longer treatment or a different therapeutic schedule of taurine might have protective effect against muscle atrophy. Previous studies on a different type of atrophy induced by dexamethasone, taurine has been shown to restore C2C12 myotube diameter, although the up-regulation of atrogin-1 was not prevented (Uozumi et al. 2006). Further experiments are thus needed to clarify the effects of taurine on muscle atrophy.

Conclusions

In conclusion, this study showed that muscle disuse induces a reduction of taurine content in postural muscles, which is likely due to a loss of the amino acid. Such an effect may have important implication for muscle function, most likely contributing to the phenotype transition and reduction of muscle strength. Supplementation of HU rats with taurine preserved many of the slow phenotype-related parameters, possibly through modulation of calcium homeostasis and protection against oxidative stress. Indeed, taurine supplementation maintained a low gCl, a high restCa, proper calcium membrane permeability through the sarcolemmal cation channels, a negative MT rheobase, and a correct distribution of MHC isoforms in HU soleus muscle. These are all key parameters/processes involved in muscle function from excitability to excitation–contraction coupling to contraction. Importantly, a number of studies have suggested that a forced fast-to-slow conversion may constitute a valuable therapeutic strategy to protect skeletal muscles in disease conditions (Schiaffino et al. 2007; Hilber 2008). A representative scheme that summarizes the HU process and taurine action is illustrated in Fig. 8. In addition, the positive effects on atrogene expression suggest that taurine might also contribute to reduce atrophy. Therefore, we propose the use of this amino acid as an adjuvant in the treatment of muscle disuse occurring in various conditions, including microgravity exposure, bed rest, and aging. It is worth noting that taurine is free of side effects thus it can be used for a long time, supporting its potential benefit also in other tissues affected by HU.

Acknowledgments Supported by research grant from the Italian Space Agency (project OSMA "Osteoporosis and Muscle Atrophy").

Conflict of interest None.

References

Adams GR, Caiozzo VJ, Baldwin KM (2003) Skeletal muscle unweighting: spaceflight and ground-based models. J Appl Physiol 95:2185–2201

Baguet A, Everaert I, Hespel P, Petrovic M, Achten E, Derave W (2011) A new method for non-invasive estimation of human muscle fiber type composition. PLoS One 6(7):e21956 Epub 7 July 2011

Bakker AJ, Berg HM (2002) Effect of taurine on sarcoplasmic reticulum function and force in skinned fast-twitch skeletal muscle fibres of the rat. J Physiol 538:185–194

Bodine SC, Latres E, Baumhueter S, Lai VK, Nunez L, Clarke BA, Poueymirou WT, Panaro FJ, Na E, Dharmarajan K, Pan ZQ, Valenzuela DM, DeChiara TM, Stitt TN, Yancopoulos GD, Glass DJ (2001) Identification of ubiquitin ligases required for skeletal muscle atrophy. Science 294:1704–1708

Bryant SH (1969) Cable properties of external intercostal muscle fibres from myotonic and nonmyotonic goats. J Physiol 204: 539–550

Bryant SH, Conte-Camerino D (1991) Chloride channel regulation in the skeletal muscle of normal and myotonic goats. Pflugers Arch 417:605–610

Canu MH, Treffort N, Picquet F, Dubreucq G, Guerardel Y, Falempin M (2006) Concentration of amino acid neurotransmitters in the somatosensory cortex of the rat after surgical or functional deafferentation. Exp Brain Res 173:623–628

Conte Camerino D, Tricarico D, Pierno S, Desaphy JF, Liantonio A, Pusch M, Burdi R, Camerino C, Fraysse B, De Luca A (2004) Taurine and skeletal muscle disorders. Neurochem Res 29:135–142

Conte Camerino D, Franconi F, Mambrini M, Bennardini F, Failli P, Bryant SH, Giotti A (1987) The action of taurine on chloride conductance and excitability characteristics of rat striated muscle fibers. Pharmacol Res Commun 19:685–701

Conte Camerino D, De Luca A, Mambrini M, Ferrannini E, Franconi F, Giotti A, Bryant SH (1989) The effects of taurine on pharmacologically induced myotonia. Muscle Nerve 12:898–904

Cozzoli A, Rolland JF, Capogrosso RF, Sblendorio VT, Longo V, Simonetti S, Nico B, De Luca A (2011) Evaluation of potential synergistic action of a combined treatment with alpha-methyl-prednisolone and taurine on the mdx mouse model of duchenne muscular dystrophy. Neuropathol Appl Neurobiol 37(3):243–256

Cuisinier C, De Michotte WJ, Verbeeck RK, Poortmans JR, Ward R, Sturbois X, Francaux M (2002) Role of taurine in osmoregulation during endurance exercise. Eur J Appl Physiol 87:489–495

Dawson R Jr, Biasetti M, Messina S, Dominy J (2002) The cytoprotective role of taurine in exercise-induced muscle injury. Amino Acids 22:309–324

De Luca A, Pierno S, Liantonio A, Cetrone M, Camerino C, Simonetti S, Papadia F, Camerino DC (2001) Alteration of excitation-contraction coupling mechanism in extensor digitorum longus muscle fibres of dystrophic mdx mouse and potential efficacy of taurine. Br J Pharmacol 132:1047–1054

Desaphy JF, Pierno S, Léoty C, George AL Jr, De Luca A, Camerino DC (2001) Skeletal muscle disuse induces fibre type-dependent enhancement of Na^+ channel expression. Brain 124:1100–1113

Desaphy JF, Pierno S, Liantonio A, De Luca A, Didonna MP, Frigeri A, Nicchia GP, Svelto M, Camerino C, Zallone A, Camerino DC (2005) Recovery of the soleus muscle after short- and long-term disuse induced by hindlimb unloading: effects on the electrical properties and myosin heavy chain profile. Neurobiol Dis 18:356–365

Desaphy JF, Pierno S, Liantonio A, Giannuzzi V, Digennaro C, Dinardo MM, Camerino GM, Ricciuti P, Brocca L, Pellegrino MA, Bottinelli R, Camerino DC (2010) Antioxidant treatment of hindlimb-unloaded mouse counteracts fiber type transition but not atrophy of disused muscles. Pharmacol Res 61:553–563

El Idrissi A (2008) Taurine increases mitochondrial buffering of calcium: role in neuroprotection. Amino Acids 34:321–328

Ferreira R, Vitorino R, Neuparth MJ, Appell HJ, Duarte JA, Amado F (2009) Proteolysis activation and proteome alterations in murine skeletal muscle submitted to 1 week of hindlimb suspension. Eur J Appl Physiol 107:553–563

Fitts RH, Riley DR, Widrick JJ (2001) Functional and structural adaptations of skeletal muscle to microgravity. J Exp Biol 204:3201–3208

Fitts RH, Romatowski JG, Peters JR, Paddon-Jones D, Wolfe RR, Ferrando AA (2007) The deleterious effects of bed rest on human skeletal muscle fibers are exacerbated by hypercortisolemia and ameliorated by dietary supplementation. Am J Physiol Cell Physiol 293:C313–C320

Fitts RH, Trappe SW, Costill DL, Gallagher PM, Creer AC, Colloton PA, Peters JR, Romatowski JG, Bain JL, Riley DA (2010) Prolonged space flight-induced alterations in the structure and function of human skeletal muscle fibres. J Physiol 588:3567–3592

Fraysse B, Desaphy JF, Pierno S, De Luca A, Liantonio A, Mitolo CI, Camerino DC (2003) Decrease in resting calcium and calcium entry associated with slow-to-fast transition in unloaded rat soleus muscle. FASEB J 17:1916–1918

Fraysse B, Desaphy J-F, Rolland J-F, Pierno S, Liantonio A, Giannuzzi V, Camerino C, Didonna MP, Cocchi D, De Luca A, Conte Camerino D (2006) Fiber type-related changes in rat skeletal muscle calcium homeostasis during aging and restoration by growth hormone. Neurobiol Dis 21:372–380

Frigeri A, Nicchia GP, Desaphy JF, Pierno S, De Luca A, Camerino DC, Svelto M (2001) Muscle loading modulates aquaporin-4 expression in skeletal muscle. FASEB J 15:1282–1284

Fujino H, Ishihara A, Murakami S, Yasuhara T, Kondo H, Mohri S, Takeda I, Roy RR (2009) Protective effects of exercise preconditioning on hindlimb unloading-induced atrophy of rat soleus muscle. Acta Physiol (Oxf) 197:65–74

Gailly P, Boland B, Himpens B, Casteels R, Gillis JM (1993) Critical evaluation of cytosolic calcium determination in resting muscle fibres from normal and dystrophic (mdx) mice. Cell Calcium 14:473–483

Gardetto PR, Schluter JM, Fitts RH (1989) Contractile function of single muscle fibers after hindlimb suspension. J Appl Physiol 66:2739–2749

Grichko VP, Heywood-Cooksey A, Kidd KR, Fitts RH (2000) Substrate profile in rat soleus muscle fibers after hindlimb unloading and fatigue. J Appl Physiol 88:473–478

Grynkiewicz G, Poenie M, Tsien RY (1985) A new generation of Ca^{2+} indicators with greatly improved fluorescence properties. J Biol Chem 260:3440–3450

Hamilton EJ, Berg HM, Easton CJ, Bakker AJ (2006) The effect of taurine depletion on the contractile properties and fatigue in fast-twitch skeletal muscle of the mouse. Amino Acids 31:273–278

Harridge SD (2007) Plasticity of human skeletal muscle: gene expression to in vivo function. Exp Physiol 92:783–797

Hilber K (2008) Skeletal myocyte plasticity: basis for improved therapeutic potential. Curr Opin Pharmacol 8:327–332

Huxtable RJ (1992) Physiological actions of taurine. Physiol Rev 72:101–163

Ito T, Kimura Y, Uozumi Y, Takai M, Muraoka S, Matsuda T, Ueki K, Yoshiyama M, Ikawa M, Okabe M, Schaffer SW, Fujio Y, Azuma J (2008) Taurine depletion caused by knocking out the taurine transporter gene leads to cardiomyopathy with cardiac atrophy. J Mol Cell Cardiol 44:927–937

Iwata H, Obara T, Kim BK, Baba A (1986) Regulation of taurine transport in rat skeletal muscle. J Neurochem 47:158–163

Kim BK, Baba A, Iwata H (1986) Taurine transport in chronically stimulated fast- and slow-twitch muscles of the rat. Jpn J Pharmacol 42:441–446

Lang F (2007) Mechanisms and significance of cell volume regulation. J Am Coll Nutr 26(5 Suppl):613S–623S

Leach CS, Alexander WC, Johnson PC (1975) Endocrine, electrolyte and fluid volume changes associated with Apollo missions. In: Biomedical results of Apollo, section III, chapter 1, http://lsda.jsc.nasa.gov/books/apollo/s3ch1.htm)

Lin J, Wu H, Tarr PT, Zhang CY, Wu Z, Boss O, Michael LF, Puigserver P, Isotani E, Olson EN, Lowell BB, Bassel-Duby R, Spiegelman BM (2002) Transcriptional co-activator PGC-1 alpha drives the formation of slow-twitch muscle fibres. Nature 418:797–801

Morey-Holton E, Globus RK, Kaplansky A, Durnova G (2005) The hindlimb unloading rat model: literature overview, technique update and comparison with space flight data. Adv Space Biol Med 10:7–40

Murton AJ, Constantin D, Greenhaff PL (2008) The involvement of the ubiquitin proteasome system in human skeletal muscle remodelling and atrophy. Biochim Biophys Acta 1782:730–743

Ojala BE, Page LA, Moore MA, Thompson LV (2001) Effects of inactivity on glycolytic capacity of single skeletal muscle fibers in adult and aged rats. Biol Res Nurs 3(2):88–95

Paddon-Jones D, Sheffield-Moore M, Urban RJ, Sanford AP, Aarsland A, Wolfe RR, Ferrando AA (2004) Essential amino acid and carbohydrate supplementation ameliorates muscle protein loss in humans during 28 days bedrest. J Clin Endocrinol Metab 89(9):4351–4358

Pasantes-Morales H, Moran J, Schousboe A (1990) Volume-sensitive release of taurine from cultured astrocytes: properties and mechanism. Glia 3(5):427–432

Pavy-Le Traon A, Heer M, Narici MV, Rittweger J, Vernikos J (2007) From space to Earth: advances in human physiology from 20 years of bed rest studies (1986–2006). Eur J Appl Physiol 101:143–194

Pedersen TH, de PF, Nielsen OB (2005) Increased excitability of acidified skeletal muscle: role of chloride conductance. J Gen Physiol 125:237–246

Pedersen TH, Macdonald WA, de Paoli FV, Gurung IS, Nielsen OB (2009) Comparison of regulated passive membrane conductance in action potential-firing fast- and slow-twitch muscle. J Gen Physiol 134(4):323–337

Pierno S, De Luca A, Camerino C, Huxtable RJ, Camerino DC (1998) Chronic administration of taurine to aged rats improves the electrical and contractile properties of skeletal muscle fibers. J Pharmacol Exp Ther 286:1183–1190

Pierno S, De Luca A, Beck CL, George AL Jr, Conte Camerino D (1999) Aging-associated down-regulation of ClC-1 expression in skeletal muscle: phenotypic-independent relation to the decrease of chloride conductance. FEBS Lett 449:12–16

Pierno S, Desaphy JF, Liantonio A, De Bellis M, Bianco G, De Luca A, Frigeri A, Nicchia GP, Svelto M, Léoty C, George AL Jr, Camerino DC (2002) Change of chloride ion channel conductance is an early event of slow-to-fast fibre type transition during unloading-induced muscle disuse. Brain 125:1510–1521

Pierno S, Desaphy JF, Liantonio A, De Luca A, Zarrilli A, Mastrofrancesco L, Procino G, Valenti G, Conte Camerino D (2007) Disuse of rat muscle in vivo reduces protein kinase C activity controlling the sarcolemma chloride conductance. J Physiol 584:983–995

Satoh H, Sperelakis N (1998) Review of some actions of taurine on ion channels of cardiac muscle cells and others. Gen Pharmacol 30:451–463

Schiaffino S, Gorza L, Sartore S, Saggin L, Ausoni S, Vianello M, Gundersen K, Lømo T (1989) Three myosin heavy chain isoforms in type 2 skeletal muscles fibres. J Muscle Res Cell Motil 10(3):197–205

Schiaffino S, Sandri M, Murgia M (2007) Activity-dependent signaling pathways controlling muscle diversity and plasticity. Physiology (Bethesda) 22:269–278

Schulte LM, Navarro J, Kandarian SC (1993) Regulation of sarcoplasmic reticulum calcium pump gene expression by hindlimb unweighting. Am J Physiol 264:C1308–C1315

Stein TP, Wade CE (2005) Metabolic consequences of muscle disuse atrophy. J Nutr 135(7):1824S–1828S

Steinmeyer K, Ortland C, Jentsch TJ (1991) Primary structure and functional expression of a developmentally regulated skeletal muscle chloride channel. Nature 354:301–304

Stevens L, Gohlsch B, Mounier Y, Pette D (1999) Changes in myosin heavy chain mRNA and protein isoforms in single fibers of unloaded rat soleus muscle. FEBS Lett 463:15–18

Talmadge RJ (2000) Myosin heavy chain isoform expression following reduced neuromuscular activity: potential regulatory mechanisms. Muscle Nerve 23:661–679

Talmadge RJ, Roy RR, Edgerton VR (1996) Distribution of myosin heavy chain isoforms in non-weight-bearing rat soleus muscle fibers. J Appl Physiol 81:2540–2546

Tappaz ML (2004) Taurine biosynthetic enzymes and taurine transporter: molecular identification and regulations. Neurochem Res 29(1):83–96

Tricarico D, Mele A, Conte Camerino D (2005) Phenotype-dependent functional and pharmacological properties of BK channels in skeletal muscle: effects of microgravity. Neurobiol Dis 20:296–302

Uozumi Y, Ito T, Hoshino Y, Mohri T, Maeda M, Takahashi K, Fujio Y, Azuma J (2006) Myogenic differentiation induces taurine transporter in association with taurine-mediated cytoprotection in skeletal muscles. Biochem J 394:699–706

Warskulat U, Flogel U, Jacoby C, Hartwig HG, Thewissen M, Merx MW, Molojavyi A, Heller-Stilb B, Schrader J, Haussinger D (2004) Taurine transporter knockout depletes muscle taurine levels and results in severe skeletal muscle impairment but leaves cardiac function uncompromised. FASEB J 18:577–579

Yang F, Li JS, Yan P, Liu YH, Wang DN (2004) Effect of taurine on NOS activity in hippocampus of rat exposed lead. Zhonghua Lao Dong Wei Sheng Zhi Ye Bing Za Zhi 22(3):203–206

Yokogoshi H, Oda H (2002) Dietary taurine enhances cholesterol degradation and reduces serum and liver cholesterol concentrations in rats fed a high-cholesterol diet. Amino Acids 23(4): 433–439

Yokogoshi H, Mochizuki H, Nanami K, Hida Y, Miyachi F, Oda H (1999) Dietary taurine enhances cholesterol degradation and reduces serum and liver cholesterol concentrations in rats fed a high-cholesterol diet. J Nutr 129(9):1705–1712

Yoshioka Y, Masuda T, Nakano H, Miura H, Nakaya S, Itazawa S, Kubokawa M (2002) In vitro 1H-NMR spectroscopic analysis of metabolites in fast- and slow-twitch muscles of young rats. Magn Reson Med Sci 1:7–13